IOP Publishing Journal of Physics: Condensed Matter
J. Phys.: Condens. Matter **34** (2022) 165602 (8pp) https://doi.org/10.1088/1361-648X/ac5199

# Excitonic condensation state in the assistance of the adiabatic and anti-adiabatic phonons

**Thi-Hong-Hai Do**[1] **and Van-Nham Phan**[2,3,*]

[1] Department of Physics, Hanoi University of Mining and Geology, Duc Thang, Bac Tu Liem, Hanoi, Vietnam
[2] Institute of Research and Development, Duy Tan University, 3 Quang Trung, Danang, Vietnam
[3] Faculty of Natural Sciences, Duy Tan University, 3 Quang Trung, Danang, Vietnam

E-mail: phanvannham@duytan.edu.vn

Received 19 November 2021, revised 20 January 2022
Accepted for publication 3 February 2022
Published 23 February 2022

**Abstract**

The excitonic condensate in semimetal and semiconducting materials with the assistance of the phonons in both the adiabatic and anti-adiabatic regimes has been investigated. In the framework of the random phase approximation, we analyse the static excitonic susceptibility function once the electrons and holes are described in the extended Falicov–Kimball model involving the electron–phonon interaction. The excitonic condensate transition point is detected as a divergence of the susceptibility function. The complex phase diagrams exhibit the significant impact of the adiabatic phonons on the stability of the excitonic condensation state. In contrast, phonons in the anti-adiabatic regime play a less role in the formation and the condensation of the excitons. Depending on the temperature or the external pressure, the excitonic condensate stability and its Bardeen–Cooper–Schrieffer–Bose–Einstein condensation crossover in the systems are also discussed in detail.

Keywords: excitonic, condensations, adiabatic, anti-adiabatic, phonons

(Some figures may appear in colour only in the online journal)

## 1. Introduction

In semimetals or semiconductors, a bosonic quasi-particle so-called exciton might be formed. That is a bound state of an electron in the conduction band and a hole in the valance band triggered by the Coulomb attraction. In such a case of sufficiently large density and low temperature, these excitons might be condensed in a macroscopic coherent quantum state like Cooper pairs in superconductors [1]. Unlike the superconducting state, the condensation state of excitons exhibits a non-conducting property and it is sometimes called an excitonic insulator state which was theoretically proposed almost 60 years ago [2–4]. Depending on whether the excitons are weakly or tightly bound, one might find either the Bardeen–Cooper–Schrieffer (BCS) or Bose–Einstein condensation (BEC) state of the excitonic condensate. Possessing a small effective mass, the excitonic condensation state is expected to be sustained at room temperature. That reason has promoted much interest of condensed matter physicists and also material scientists in studying the excitonic condensation state.

In general, the excitonic condensation state is foremost investigated in purely electronic models, i.e., only the Coulomb interaction between the electron and hole is considered [2–8]. However, recent several experiments have indicated that the lattice distortions also play important roles to anticipate the excitonic condensation state [9–11]. For instance, in the pressure-sensitive mixed valence material $TmSe_{0.45}Te_{0.55}$, the excitonic condensation state is found in accompanying with an abrupt change of lattice displacement [12]. Or in $1T$–$TiSe_2$ transition-metal dichalcogenides, the

* Author to whom any correspondence should be addressed.

 

charge-density-wave is observed as a driving force of the condensation of the excitons [13, 14]. Most recently, one has revealed a record critical temperature of the excitonic condensate up to $T_c = 326$ K in $Ta_2NiSe_5$, a direct gap semimetal with Ta 5*d* conduction bands and Ni 3*d* valence bands [15]. The transition is accompanied by a slight shear distortion that reduces the lattice symmetry from orthorhombic to monoclinic [11, 15]. In the last case, a strong electron–phonon coupling has been manifested to mediate the excitonic condensation state [11, 16, 17]. From the experimental observations above, considering the electron–phonon interaction is crucially important to underline physics of the excitonic condensation state in semimetal/semiconductor materials. In our work here, both the Coulomb interaction between the electrons and the holes and the electron–hole excitation phonon coupling would be considered to examine their contributions to the stability of the excitonic condensation state.

Taking into account the phonon assistance mediating the underlying physics of electronic systems, the energy level of the phonons in relativity with that of electrons is a crucial parameter specifying the signature of the lattice degree of freedoms. Depending on a comparison of the mobility of the phonons with that of electrons, one often sorts the two regimes so-called adiabatic and anti-adiabatic limits corresponding to whether the bare electronic hopping is either sufficiently small (anti-adiabatic) or sufficiently large (adiabatic) as compared to the phonon frequency. In the anti-adiabatic limit, all phonon excitations are out of the conduction band and only the electronic excitations remain active at low temperatures. In contrast, there is a strong mixing between the electronic and phononic properties in the adiabatic regime. Analysing the competition between the phonon and the electron mobilities is thus essential in the electron–phonon problem. In the polarization-resolved Raman spectroscopy experiments, one has specified the strong variation of the phonon frequencies in the excitonic insulator compositions $Ta_2Ni(Se_{1-x}S_x)_5$ [18]. Indeed, for $x < 0.7$ the semimetal compositions exhibit the pronouncedly harden phonon upon cooling in the vicinity of the excitonic condensation critical temperature. In contrast, the monotonically soften phonon is found for semiconducting situations, i.e., at $x = 1$. Subedi, recently by using the density functional theory, has revealed a large range of phonon frequencies (from 30 to 280 ($cm^{-1}$) suggesting that the wide range frequency zone-center optical phonon instability mediates the excitonic condensate phase transition in $Ta_2NiSe_5$ [19]. In the present work, we examine in detail the instability of the excitonic condensate in the wide range of the phonon frequency in the competition with the hopping parameter of conduction electrons, i.e., in both the anti-adiabatic and adiabatic limitations.

From the motivations addressed above, in this paper, the excitonic condensation state in the semimetals/semiconductors is considered in the scenario of the extended Falicov–Kimball model (EFKM) involving the electron–phonon interaction. Within the EFKM, an $f$-valance electron is not localized but disperses in a narrow band that might hybridize with the $c$-electron in the conduction band to establish the electron–hole excitations. The EFKM its own has been extensively investigated to discuss the excitonic condensate instability in almost semimetal/semiconducting materials [6, 7, 20, 21]. However, in these studies, the lattice degree of freedoms is not taken into account. Taking into account the coupling of the electron–hole excitations to the phonons, more realistic excitonic condensate signatures might be modelled and its results might explain the experimental observations. Recently, the EFKM in accompanying with the electron–phonon coupling has also been adopted to discuss the excitonic condensation state [14, 22, 23]. In these studies, the condensate phase is specified in the signatures of the excitonic order parameter only and the excitonic fluctuations especially in the vicinity of the critical point are not considered. In the meanwhile, the excitonic fluctuation at a large temperature is a crucial point to address the stability of the excitonic condensation state in the low temperature range [24, 25]. In the present work, the excitonic fluctuations in the EFKM with electron–phonon coupling will be analysed in the random phase approximation. The phase diagrams of the excitonic condensate then would be figured out in signatures of the excitonic susceptibility function. BCS–BEC crossover of the condensation state is also specified by analysing the momentum distribution of the excitonic order parameters. That is indeed essential because whether the formation of the excitonic condensation state in the materials follows the BCS or the BEC type, especially in the materials with strong electron–phonon interaction, is still in debated [15, 26].

This paper is organized as follows. In section 2, we introduce the Hamiltonian of the EFKM involving electron–phonon interaction in the momentum space. Analytical calculations for excitonic order parameters and susceptibility functions in the mean-field scheme are respectively briefly outlined in sections 3 and 4. Numerical results are given in section 5, where phase diagrams of the excitonic condensation state are addressed. In the final section, we present the conclusions.

## 2. Hamiltonian

To inspect the microscopic features of the electron–hole phonon system we introduce, in this section, the following Hamiltonian

$$\mathcal{H} = \mathcal{H}_e^0 + \mathcal{H}_{ph}^0 + \mathcal{H}_{int}, \tag{1}$$

where the non-interacting part, the first two terms $\mathcal{H}_e^0$ and $\mathcal{H}_{ph}^0$, indicates the kinetic energy of the electron–hole phonon system. The last term, $\mathcal{H}_{int}$, is its interacting part. In the momentum space, $\mathcal{H}_e^0$ reads

$$\mathcal{H}_e^0 = \sum_{\mathbf{k}} \varepsilon_{\mathbf{k}}^f f_{\mathbf{k}}^\dagger f_{\mathbf{k}} + \sum_{\mathbf{k}} \varepsilon_{\mathbf{k}}^c c_{\mathbf{k}}^\dagger c_{\mathbf{k}}. \tag{2}$$

Here, $f_{\mathbf{k}}^\dagger(f_{\mathbf{k}})$ and $c_{\mathbf{k}}^\dagger(c_{\mathbf{k}})$ respectively denote the creation (annihilation) operators of the $f$ electrons in the valence band and the $c$ electrons in the conduction band carrying momentum $\mathbf{k}$ with the electronic dispersion relation in the tight-binding

approximation

$$\varepsilon_{\mathbf{k}}^{f(c)} = \varepsilon^{f(c)} - t^{f(c)}\gamma_{\mathbf{k}} - \mu, \tag{3}$$

with the on-site energy $\varepsilon^{f(c)}$. In equation (3), $t^{f(c)}$ is the nearest-neighbor hopping amplitude of the $f(c)$ electrons and $\gamma_{\mathbf{k}} = 2\left(\cos k_x + \cos k_y\right)$ in the 2D systems. $\mu$ is the chemical potential. In the momentum space, $\mathcal{H}_{\rm ph}^0$ also reads

$$\mathcal{H}_{ph}^0 = \omega_0 \sum_{\mathbf{q}} b_{\mathbf{q}}^\dagger b_{\mathbf{q}}, \tag{4}$$

where $b_{\mathbf{q}}^\dagger(b_{\mathbf{q}})$ is phonon creation (annihilation) operator at momentum $\mathbf{q}$ and $\omega_0$ is dispersionless single mode phonon energy. Here the longitudinal optical phonons are represented in the Einstein model in which the phonon frequency is momentum independent. Comparing the phonon frequency $\omega_0$ with the conduction electron hopping term $t^c$, one can sort two typical limitations: adiabatic ($\omega_0 < t^c$) and anti-adiabatic $\omega_0 > t^c$ with respect to higher and less mobility of the phonons than that of the electrons.

In the electron–hole phonon system, the interaction part $\mathcal{H}_{\rm int}$ includes both the Coulomb interaction between $c$ and $f$ electrons and the electron–phonon interaction between the $f$–$c$ electron excitations with the lattice displacements. In the $\mathbf{k}$ space, it is written by

$$\mathcal{H}_{\rm int} = \frac{U}{N}\sum_{k,k',q} c_{\mathbf{k}+q}^\dagger c_{k'} f_{\mathbf{k}'-q}^\dagger f_{\mathbf{k}} + \frac{g}{\sqrt{N}}\sum_{\mathbf{kq}}\left[c_{\mathbf{k}+\mathbf{q}}^\dagger f_{\mathbf{k}}\left(b_{-\mathbf{q}}^\dagger + b_{\mathbf{q}}\right) + \text{H.c.}\right], \tag{5}$$

where $N$ is the number of lattice sites. Here, we have assumed that both the interactions are local with respect to $U$ being the Coulomb attraction intensity and $g$ being the electron–phonon coupling constant. Note here that the Hamiltonian written in equation (1) deals with a closed exciton–phonon system. In experiments, the excitonic system is usually performed away from equilibrium. Considering the excitonic condensation state in the influence of the environment is thus very important and more realistic. The task for the non-equilibrium situation will be left for future studies.

## 3. The unrestricted Hartree–Fock approximation

The Hamiltonian written in equation (1) captures many-body features and it is difficult to be exactly solved. In the present work, the Hamiltonian is simply examined in the unrestricted Hartree–Fock approximation (UHFA). In the UHFA, all fluctuation parts are eliminated and the problem reduces to a single-particle feature. The effective Hamiltonian then is written as

$$\mathcal{H}_{\rm eff} = \sum_{\mathbf{k}} \bar{\varepsilon}_{\mathbf{k}}^f f_{\mathbf{k}}^\dagger f_{\mathbf{k}} + \sum_{\mathbf{k}} \bar{\varepsilon}_{\mathbf{k}}^c c_{\mathbf{k}}^\dagger c_{\mathbf{k}} + \Lambda\sum_{\mathbf{k}}\left(c_{\mathbf{k}+\mathbf{q}}^\dagger f_{\mathbf{k}} + \text{H.c.}\right) + \omega_0\sum_{\mathbf{q}} b_{\mathbf{q}}^\dagger b_{\mathbf{q}} + \sqrt{N}h(b_{-\mathrm{q}}^\dagger + b_{\mathbf{q}}). \tag{6}$$

Here the Coulomb interaction contribution in the approximation so-called the Hartree shifts has been involved to the electronic excitation energies

$$\bar{\varepsilon}_{\mathbf{k}}^{c(f)} = \varepsilon_{\mathbf{k}}^{c(f)} + Un^{f(c)}, \tag{7}$$

where $n^{f(c)} = \sum_{\mathbf{k}}\langle n_{\mathbf{k}}^{f(c)}\rangle/N$ is the $f(c)-$electron density, with the denotations $\langle n_{\mathbf{k}}^f\rangle = \langle f_{\mathbf{k}}^\dagger f_{\mathbf{k}}\rangle$ and $\langle n_{\mathbf{k}}^c\rangle = \langle c_{\mathbf{k}}^\dagger c_{\mathbf{k}}\rangle$. $\Lambda$ and $h$ in the effective Hamiltonian $\mathcal{H}_{\rm eff}$ are the additional fields given by

$$h = \frac{g}{N}\sum_{\mathbf{k}}\langle c_{\mathbf{k}+\mathbf{q}}^\dagger f_{\mathbf{k}} + \text{H.c.}\rangle, \tag{8}$$

$$\Lambda = \frac{g}{\sqrt{N}}\langle b_{-\mathbf{q}}^\dagger + b_{\mathbf{q}}\rangle - \frac{U}{N}\sum_{\mathbf{k}}\langle c_{\mathbf{k}+\mathbf{q}}^\dagger f_{\mathbf{k}}\rangle, \tag{9}$$

are considered to be the excitonic condensate order parameters. Here, we have assumed that only the excitons mediated by the phonons with momentum $\mathbf{q}$ are considered. That might be condensed indicating by the non-zero expectation value $\langle c_{\mathbf{k}+\mathbf{q}}^\dagger f_{\mathbf{k}}\rangle$.

The effective Hamiltonian in equation (6) needs to be diagonalized then the expectation values in equations (7)–(9) could be evaluated. The equations to determine self-consistently the electron densities and excitonic order parameters can be found in reference [22]. In the case out of the excitonic condensation, all excitonic condensate order parameters are vanished or both $h$ and $\Lambda$ in equation (6) are zero. The effective Hamiltonian becomes very simple and the electron densities are easily evaluated. One has

$$\langle n_{\mathbf{k}}^{f(c)}\rangle = \frac{1}{1 + e^{\beta\bar{\varepsilon}_{\mathbf{k}}^{f(c)}}}, \tag{10}$$

with $\beta = 1/T$ and $T$ is the temperature.

## 4. Excitonic susceptibility function

To consider the stability of the excitonic condensation state, in this paper, we analyse the excitonic susceptibility possibly creating an bound state of electron–hole pair carrying momentum $\mathbf{q}$ at large temperature

$$\chi(\mathbf{q},\omega) = -\langle\langle X_{\mathbf{q}}|X_{\mathbf{q}}^\dagger\rangle\rangle_\omega, \tag{11}$$

where $X_{\mathbf{q}}^\dagger$ is the electron–hole excitation creation operator with momentum $\mathbf{q}$ and $\langle\langle\cdots\rangle\rangle$ denotes the retarded Green function in the frequency representation. In our problem, the electron–hole excitation creation operator with momentum $\mathbf{q}$ is $X_{\mathbf{q}}^\dagger = \frac{1}{\sqrt{N}}\sum_{\mathbf{k}} c_{\mathbf{k}+\mathbf{q}}^\dagger f_{\mathbf{k}}$ then the momentum and frequency dependence of the excitonic susceptibility can be read

$$\chi(\mathbf{q},\omega) = -\frac{1}{N}\sum_{\mathbf{kk}'}\langle\langle f_{\mathbf{k}}^\dagger c_{\mathbf{k}+\mathbf{q}}|c_{\mathbf{k}'+\mathbf{q}}^\dagger f_{\mathbf{k}'}\rangle\rangle_\omega. \tag{12}$$

For the Hamiltonian $\mathcal{H}$ written in equation (1), the two-particle Green's function in the sum of equation (12) can be evaluated, such as following the equation of motion

$$\omega\langle\langle f^{\dagger}_{\mathbf{k}}c_{\mathbf{k}+\mathbf{q}}|c^{\dagger}_{\mathbf{k}'+\mathbf{q}}f_{\mathbf{k}'}\rangle\rangle_{\omega} = \langle[f^{\dagger}_{\mathbf{k}}c_{\mathbf{k}+\mathbf{q}}; c^{\dagger}_{\mathbf{k}'+\mathbf{q}}f_{\mathbf{k}'}]\rangle + \langle\langle[f^{\dagger}_{\mathbf{k}}c_{\mathbf{k}+\mathbf{q}}; \mathcal{H}]|c^{\dagger}_{\mathbf{k}'+\mathbf{q}}f_{\mathbf{k}'}\rangle\rangle_{\omega}. \tag{13}$$

It results

$$\begin{aligned}\omega\langle\langle f^{\dagger}_{\mathbf{k}}c_{\mathbf{k}+\mathbf{q}}|c^{\dagger}_{k'+q}f_{k'}\rangle\rangle_{\omega} &= \langle n^{f}_{\mathbf{k}}\rangle - \langle n^{c}_{\mathbf{k}+\mathbf{q}}\rangle \\ &+ (\varepsilon^{c}_{\mathbf{k}+\mathbf{q}} - \varepsilon^{f}_{\mathbf{k}})\langle\langle f^{\dagger}_{\mathbf{k}}c_{\mathbf{k}+\mathbf{q}}|c^{\dagger}_{k'+q}f_{k'}\rangle\rangle_{\omega} \\ &+ \frac{U}{N}\sum_{k''q_1}\Big\langle\Big\langle\Big(f^{\dagger}_{\mathbf{k}}c_{k''}f^{\dagger}_{\mathbf{k}''-q_1}f_{\mathbf{k}+\mathbf{q}-\mathbf{q}_1} \\ &- c^{\dagger}_{\mathbf{k}+\mathbf{q}_1}c_{k''}f^{\dagger}_{\mathbf{k}''-q_1}c_{\mathbf{k}+\mathbf{q}}\Big)|c^{\dagger}_{k'+q}f_{k'}\Big\rangle\Big\rangle_{\omega} \\ &+ \frac{g}{\sqrt{N}}\sum_{\mathbf{q}_1}\Big\langle\Big\langle(f^{\dagger}_{\mathbf{k}}f_{\mathbf{k}+\mathbf{q}-\mathbf{q}_1} - c^{\dagger}_{\mathbf{k}+\mathbf{q}_1}c_{\mathbf{k}+\mathbf{q}}) \\ &\times (b^{\dagger}_{-\mathbf{q}_1} + b_{\mathbf{q}_1})|c^{\dagger}_{k'+q}f_{k'}\Big\rangle\Big\rangle_{\omega}. \end{aligned} \tag{14}$$

Here, the electron densities are given in equation (10). In the random phase approximation, the excess operators in the higher order Green's functions can be factorized and one might approximate

$$\begin{aligned}\sum_{\mathbf{k}''\mathbf{q}_1}\langle\langle f^{\dagger}_{\mathbf{k}}c_{\mathbf{k}''}f^{\dagger}_{\mathbf{k}''-\mathbf{q}_1}f_{\mathbf{k}+\mathbf{q}-\mathbf{q}_1}|c^{\dagger}_{\mathbf{k}'+\mathbf{q}}f_{\mathbf{k}'}\rangle\rangle_{\omega} &\approx \sum_{\mathbf{q}_1}\langle n^{f}_{\mathbf{k}+\mathbf{q}-\mathbf{q}_1}\rangle\langle\langle f^{\dagger}_{\mathbf{k}}c_{\mathbf{k}+\mathbf{q}}|c^{\dagger}_{\mathbf{k}'+\mathbf{q}}f_{\mathbf{k}'}\rangle\rangle_{\omega} \\ &- \sum_{\mathbf{k}_2}\langle n^{f}_{\mathbf{k}}\rangle\langle\langle f^{\dagger}_{\mathbf{k}_2}c_{\mathbf{k}_2+\mathbf{q}}|c^{\dagger}_{\mathbf{k}'+\mathbf{q}}f_{\mathbf{k}'}\rangle\rangle_{\omega}, \end{aligned} \tag{15}$$

and

$$\begin{aligned}\sum_{\mathbf{k}''\mathbf{q}_1}\langle\langle c^{\dagger}_{\mathbf{k}+\mathbf{q}_1}c_{\mathbf{k}''}f^{\dagger}_{\mathbf{k}''-\mathbf{q}_1}c_{\mathbf{k}+\mathbf{q}}|c^{\dagger}_{\mathbf{k}'+\mathbf{q}}f_{\mathbf{k}'}\rangle\rangle_{\omega} &\approx \sum_{\mathbf{q}_1}\langle n^{c}_{\mathbf{k}+\mathbf{q}_1}\rangle\langle\langle f^{\dagger}_{\mathbf{k}}c_{\mathbf{k}+\mathbf{q}}|c^{\dagger}_{\mathbf{k}'+\mathbf{q}}f_{\mathbf{k}'}\rangle\rangle_{\omega} \\ &- \sum_{\mathbf{k}_2}\langle n^{c}_{\mathbf{k}+\mathbf{q}}\rangle\langle\langle f^{\dagger}_{\mathbf{k}_2}c_{\mathbf{k}_2+\mathbf{q}}|c^{\dagger}_{\mathbf{k}'+\mathbf{q}}f_{\mathbf{k}'}\rangle\rangle_{\omega}, \end{aligned} \tag{16}$$

and in similarly, one obtains

$$\begin{aligned}\sum_{\mathbf{q}_1}\langle\langle f^{\dagger}_{\mathbf{k}}f_{\mathbf{k}+\mathbf{q}-\mathbf{q}_1}(b^{\dagger}_{-\mathbf{q}_1} + b_{\mathbf{q}_1})|c^{\dagger}_{\mathbf{k}'+\mathbf{q}}f_{\mathbf{k}'}\rangle\rangle_{\omega} &\approx \langle n^{f}_{\mathbf{k}}\rangle\langle\langle(b^{\dagger}_{-\mathbf{q}} + b_{\mathbf{q}})|c^{\dagger}_{\mathbf{k}'+\mathbf{q}}f_{\mathbf{k}'}\rangle\rangle_{\omega}, \end{aligned} \tag{17}$$

and

$$\begin{aligned}\sum_{\mathbf{q}_1}\langle\langle c^{\dagger}_{\mathbf{k}+\mathbf{q}_1}c_{\mathbf{k}+\mathbf{q}}(b^{\dagger}_{-\mathbf{q}_1} + b_{\mathbf{q}_1})|c^{\dagger}_{\mathbf{k}'+\mathbf{q}}f_{\mathbf{k}'}\rangle\rangle_{\omega} &\approx \langle n^{c}_{\mathbf{k}+\mathbf{q}}\rangle\langle\langle(b^{\dagger}_{-\mathbf{q}} + b_{\mathbf{q}})|c^{\dagger}_{\mathbf{k}'+\mathbf{q}}f_{\mathbf{k}'}\rangle\rangle_{\omega}. \end{aligned} \tag{18}$$

Note that here we are dealing with out side of the excitonic condensation state, all the terms multiplying with the excitonic order parameters or the lattice distortion are completely eliminated. In the same manner, one also delivers

$$\langle\langle(b^{\dagger}_{-\mathbf{q}} + b_{\mathbf{q}})|c^{\dagger}_{\mathbf{k}+\mathbf{q}}f_{\mathbf{k}}\rangle\rangle_{\omega} = \frac{\Gamma_{\mathbf{q}}}{\sqrt{N}}\sum_{\mathbf{k}_1}\langle\langle f^{\dagger}_{\mathbf{k}_1}c_{\mathbf{k}_1+\mathbf{q}}|c^{\dagger}_{\mathbf{k}+\mathbf{q}}f_{\mathbf{k}}\rangle\rangle_{\omega}, \tag{19}$$

where

$$\Gamma_{\mathbf{q}} = \frac{2g\omega_0}{\omega^2 - \omega_0^2 - \frac{2g^2\omega_0\chi^{0b}(\mathbf{q},\omega)}{1+U\chi^{0b}(\mathbf{q},\omega)}}, \tag{20}$$

with a denotation

$$\chi^{0b}(\mathbf{q},\omega) = \frac{1}{N}\sum_{\mathbf{k}}\frac{\langle n^{c}_{\mathbf{k}-\mathbf{q}}\rangle - \langle n^{f}_{\mathbf{k}}\rangle}{\omega - \bar{\varepsilon}^{f}_{\mathbf{k}} + \bar{\varepsilon}^{c}_{\mathbf{k}-\mathbf{q}}}. \tag{21}$$

In the help of equation (19), one derives a final expression of the excitonic susceptibility function for the Hamiltonian written in equation (1), that reads

$$\chi(\mathbf{q},\omega) = \frac{-\chi^{0}(\mathbf{q},\omega)}{1 + (U - g\Gamma_{\mathbf{q}})\chi^{0}(\mathbf{q},\omega)}, \tag{22}$$

where

$$\chi^{0}(\mathbf{q},\omega) = \frac{1}{N}\sum_{\mathbf{k}}\frac{\langle n^{f}_{\mathbf{k}}\rangle - \langle n^{c}_{\mathbf{k}+\mathbf{q}}\rangle}{\omega - \bar{\varepsilon}^{c}_{\mathbf{k}+\mathbf{q}} + \bar{\varepsilon}^{f}_{\mathbf{k}}}, \tag{23}$$

plays a role of the bare electron–hole susceptibility function.

To establish phase diagrams of the excitonic condensation state in the Hamiltonian (1), in the present work, we analyse the static excitonic susceptibility function, i.e., $\chi(\mathbf{q},\omega)$ in equation (22) at $\omega \to 0$. The static excitonic susceptibility represents the excitonic fluctuation in the system. The stability of the excitonic condensation state thus might be pointed out by the divergence of the excitonic susceptibility function.

## 5. Numerical results and discussion

To inspect the excitonic condensation state instability in semimetal/semiconducting materials, in this section, we address the numerical results based on the analytical calculations above. The numerical calculation proceeds for a 2D system containing $N = 500 \times 500$ lattice sites and the set of self-consistent equations equations (7) and (10) is solved to determine the expected values. The static excitonic susceptibility function $\chi(\mathbf{q})$ in equation (22) at $\omega \to 0$ is then evaluated. Without loss of the generality, $t^{c} = 1$ is chosen as the unit of energy and the results are fixed for the case of $t^{f} = -0.3$ and $\varepsilon^{c} = 0$. The choice of $t^{f}$ indicates the direct band-gap situation, i.e., the valence-band maximum and the conduction-band minimum simultaneously locate at the Brillouin-zone center. That situation is reasonable to the semimetal $Ta_2NiSe_5$ that reveals the record critical temperature of the excitonic condensate driven by the strong electron–phonon coupling.

Firstly, we display in figure 1 the momentum dependence of the static excitonic susceptibility as a function of temperature. For a given set of parameters, one sees that the susceptibility function diverges at zero-momentum and then suddenly drops down for the momenta deviating from zero. The divergence indicates that the excitons with zero-momentum become most favoured in the situation and the ordering vector of the

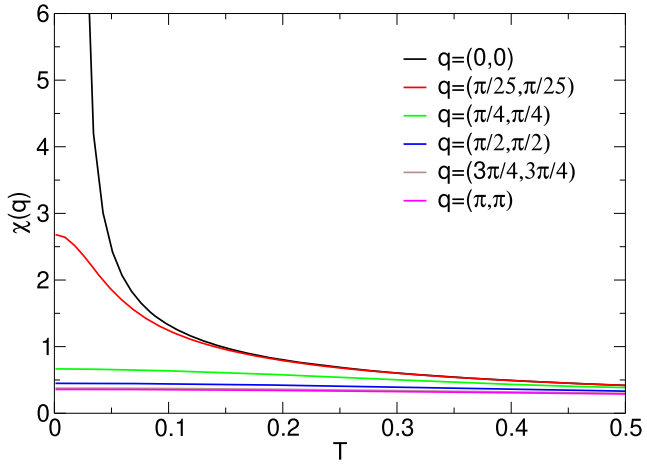


**Figure 1.** The static excitonic susceptibility $\chi(\mathbf{q})$ as a function of temperature $T$ for some values of momenta $\mathbf{q}$ at $U = 0.4$, $g = 0.3$, $\varepsilon^f = -2.0$, and $\omega_0 = 0.5$.

low-temperature phase is $\mathbf{q} = \mathbf{0}$. That is a situation of the excitons in the semimetal $Ta_2NiSe_5$ observed recently [11, 16, 17]. Hereafter, we will consider the excitonic susceptibility function for the zero-momentum case only to discuss the instability of the excitonic condensation state.

To detect the excitonic condensate in the system, normally one discusses the properties of the excitonic order parameters. For a comparison, in figure 2 we show a temperature dependence of both the excitonic condensate order parameter $\Lambda$ (symbol-lines) and the static excitonic susceptibility function $\chi$ (solid lines) for difference $g$ at given $\varepsilon^f = -2.0$ and $U = 0.4$ in the two adiabatic ($\omega_0 = 0.5$) and anti-adiabatic ($\omega_0 = 5$) limitations. In both regimes, one might find the nonzero values of the order parameter at low temperature specifying the stability of the excitonic condensation state if the electron–phonon coupling is large enough. Increasing temperature, the thermal fluctuations destroy a part of the $c - f$ electronic bounding state and thus the condensation state is depressed. That is indicated by the depression of the excitonic order parameter. Once the temperature is sufficiently large, the order parameter is completely disappeared and the system is out of the order state. The temperature at which the order parameter suddenly drops down to zero is so-called the excitonic condensate transition temperature $T_c$. For a given small Coulomb coupling, the electron–hole pairs might be formed if the electron–phonon coupling is large enough. Increasing the electron–phonon coupling the hybridization between the electrons and holes is enhanced. The bound electron–hole excitations become more stable. The behaviours of the excitonic properties seem to be unchanged in both regimes of the phonon frequencies. However, in the adiabatic regime, the phonon energy is small, the dynamic signature of the phonons is comparable to that of the electrons, and hence, the electron–phonon correlations are reinforced even at a small electron–phonon interaction [see figure 2(a)]. On the other hand, in the anti-adiabatic regime, the phonon level is even above the highest level of the conduction band. The electron–phonon interaction thus must be extremely large to establish the bound excitonic–phonon excitations to stabilize the condensation state [see figure 2(b)].

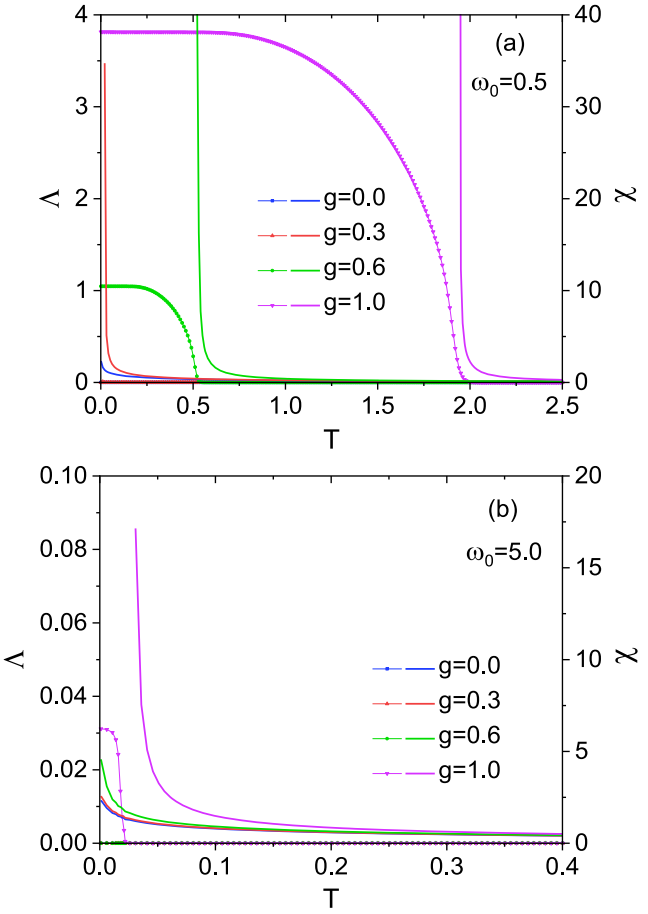


**Figure 2.** The static excitonic susceptibility $\chi$ at zero-momentum (solid lines) and the excitonic condensate order parameter $\Lambda$ (symbol-lines) as functions of the temperature $T$ for different values of $g$ at $\varepsilon^f = -2.0$ and $U = 0.4$ with the phonon frequencies $\omega_0 = 0.5$ (a) and $\omega_0 = 5.0$ (b).

Analysing the order parameter thus might establish the phase structure of the excitonic condensation state. However, the excitonic order parameter only addresses the dynamic properties of the condensate at a temperature smaller than the critical value. Investigating the dynamic properties of the electron–hole excitations in the signatures of the static excitonic susceptibility function above the transition temperature hence is essential. Indeed, in all cases, one always finds the development of the static susceptibility function as decreasing the temperature (see solid lines in figure 2). For the temperature close to the critical value, the susceptibility function sharply enlarges and then diverges at $T = T_c$, $T_c$ is indicated to the excitonic transition temperature. The accession of the susceptibility as decreasing temperature illustrates the enhancement of the electron–hole bound state excitations against the thermal fluctuations. Increasing the electron–phonon coupling also provides strong evidence for the development of the excitonic fluctuations. Absolutely, in the adiabatic regime, the phonon strongly mediates the excitonic bound excitation states, the excitonic fluctuations thus are enhanced in comparison to the case in the anti-adiabatic regime.

To describe in more detail the effects of the phonon frequency on the formation of the excitonic condensate state in

the system, we display in figure 3 the ground-state phase diagrams in the $(U, \omega_0)$ plane for different values of the electron–phonon coupling $g$ at the $f$-electron one-site energy $\varepsilon^f = -2.0$. Our phase diagrams are constructed by detecting the divergence of the static excitonic susceptibility. We see that for a given value of $g$ and a fixed $\omega_0$, the excitonic condensation phase is established as the Coulomb interaction is in a range of $U_{c1} < U < U_{c2}$. For $U < U_{c1}$, both the Coulomb interaction and electron–phonon coupling are not strong enough to pair electrons and holes, and the system settles in the semimetal state. On the other hand, for $U > U_{c2}$, the band-gap due to the Hartree shift excludes the hybridization between conduction and valance band, and thus the system is also out of the order state. The system, instead, settles in the semiconductor side. As increasing the phonon frequency $\omega_0$, $U_{c1}$ increases whereas $U_{c2}$ decreases, the condensed region of excitons, therefore, is depressed. This results the consistency of our findings with that of the experimental observations on the material $Ta_2NiSe_5$ by using Raman spectroscopy with soft phonon modes [27]. In which, the low-energy optical phonons play a role in promoting the transition to the excitonic condensation state. Growing electron–phonon interaction, the excitonic condensate window is expanded. Indeed, for a very small electron–phonon coupling, for instance $g = 0.01$, the excitonic condensation state is established in the narrow region of the Coulomb interaction (see figure 3(a)). When the electron–phonon interaction increases, $U_{c1}$ decreases and $U_{c2}$ increases, that makes enlarge the excitonic condensate regime in the plane [see figures 3(b)–(d)]. In particular, for sufficiently large $g$, the excitonic condensation phase can be formed even for $U = 0$ at a small phonon frequency. In this case, the condensation of excitons in the system is entirely due to the electron–phonon coupling, which has been discussed in references [28–31]. In the figure 3, the phonon frequency has illustrated a significant effect in the excitonic condensate. Indeed, for low phonon frequency, the dynamic of the phonon is comparable with that of the electrons, thus the electron–phonon correlations become prominent. The excitonic condensate hence might be stabilized even without the Coulomb interaction. A slight change of the phonon frequency in this regime also delivers a significant alteration of the exciton excitations. This has been demonstrated experimentally in $Ta_2NiSe_5$ in which the structural phase transition from orthorhombic to monoclinic structural is driven by the softening of optical phonon mode [27, 32]. For a large phonon frequency, the phonon level is far from the Fermi level and thus it might be less important to impact the excitonic excitations. Varying the phonon frequency in this situation is therefore insignificant to the stability of the excitonic condensation state. The excitonic condensate in the anti-adiabatic case thus is primarily driven by the Coulomb interaction only. Indeed, for infinite phonon frequency, the phase boundary would recover the situation of the purely electronic systems.

Depending on the strength of the interactions, the excitons can be stabilized in the either BCS or BEC-type condensation state if the bound electron–hole pairs are weak or tight. In the figure 3 both the BCS and BEC-type of the excitonic

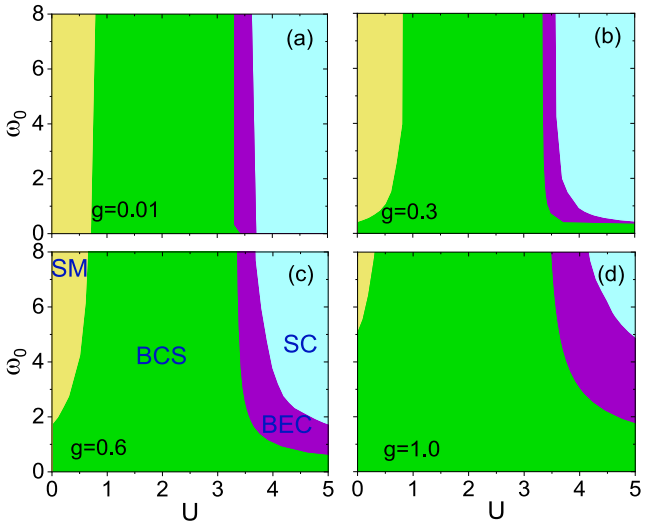


**Figure 3.** Ground-state phase diagrams of the excitonic condensation state in the $(U, \omega_0)$ plane for some values of $g$ at $\varepsilon^f = -2.0$. The excitonic condensate being in BCS-type and BEC-type are indicated by green- and purple-region, respectively. The semimetal/semiconducting state is pointed out by the yellow/blue region.

condensate are specified. On the BCS side, the excitonic condensation state is driven by the small interactions between electrons and holes in the semimetal state. The two valance and conduction bands are overlapped and only the electrons and holes near the Fermi surface build up the excitons. In this case, the electron–hole pair distribution $\langle c^\dagger_{\mathbf{k}+\mathbf{q}} f_{\mathbf{k}} \rangle$ peaks at a finite Fermi momentum. Otherwise, with the strong interactions in the semiconducting side, the tightly bound excitons might be formed. They act as a diluted neutral gas and thus one finds the BEC excitonic condensation state. In this situation, the Fermi surface plays no role in the formation of the excitons. The pair distribution thus peaks at zero momentum. For this feature, the BCS–BEC crossover of the excitonic condensation state is addressed. Figure 3 shows us that growing the electron–phonon coupling moves the BCS–BEC crossover to the larger Coulomb interaction regime. The effect of the phonon frequency is also found significantly in the adiabatic regime for the intermediate electron–phonon interaction.

In that manner, we show in figure 4 the ground-state phase diagrams of the excitonic condensate in the $(U, \varepsilon^f)$ plane for different phonon frequencies $\omega_0$ at a given electron–phonon coupling $g = 0.6$. Due to the choice with $\varepsilon^c = 0$, the onsite energy $\varepsilon^f$ represents the overlap between the $f$- and the $c$-bands, measuring the possible coupling between the electrons and the holes to form the excitons caused by the external pressure [9, 33]. At a given phonon frequency, we always find the excitonic condensation state for small $|\varepsilon^f|$. Two $f$- and $c$-bands, in this case, are strongly overlapped and the system settles in the BCS-type excitonic condensate. That type of the condensation is depressed in the case of small Coulomb interaction in anti-adiabatic regime [see figures 4(c) and (d)]. In that situation, the contribution of the phonons becomes less important and if the Coulomb interaction is not sufficiently large, electrons and holes would not be bound to form a pair and one finds only the semimetal state. In the adiabatic regime,

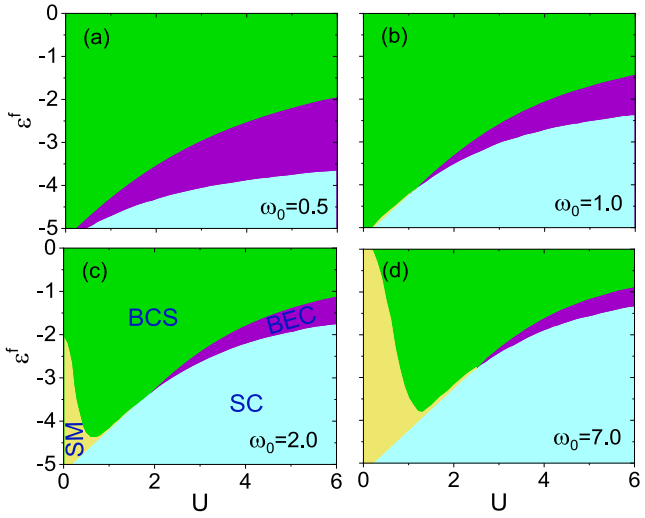


**Figure 4.** Ground-state phase diagrams of the excitonic condensation state in the $(U, \varepsilon^f)$ plane for different phonon frequencies $\omega_0$ at $g = 0.6$. The excitonic condensate being in BCS-type and BEC-type are indicated by green- and purple-region, respectively. The semimetal/semiconducting state is pointed out by the yellow/blue region.

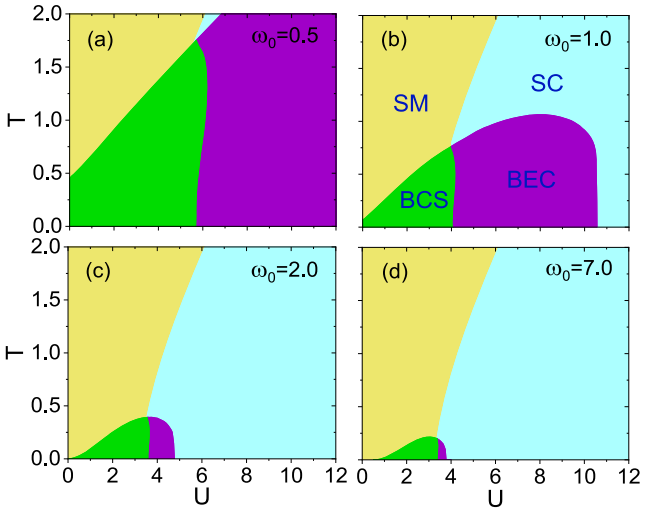


**Figure 5.** Phase diagrams of the excitonic condensation state in the $(U, T)$ plane for some $\omega_0$ at $\varepsilon^f = -2.0$ and $g = 0.6$. The excitonic condensate being in BCS-type and BEC-type that are indicated by green- and purple-region, respectively. The semimetal/semiconducting state is pointed out by the yellow/blue region.

otherwise, the condensation state can be found even without the Coulomb interaction. That condensation state might be driven barely by the electron–phonon coupling when the entanglement between electrons and phonons is significant [see figures 4(a) and (b)]. In the whole regime of the phonon frequency, the BEC excitonic condensate is always stabilized for large Coulomb interaction.

To address the thermal fluctuations affecting the complex phase structure in the systems, in figure 5 we show the phase diagrams in the $(U, T)$ plane for different phonon frequencies $\omega_0$ at the given set of parameters $\varepsilon^f = -2.0$ and $g = 0.6$. The boundary shape of the condensation state seems to be unchanged for all phonon frequencies $\omega_0$. However, the amplitude of the transition temperature is rapidly suppressed once the system enters the anti-adiabatic regime. For an appropriate Coulomb interaction, one always finds the excitonic condensation state at low temperature. Enlarging temperature, the thermal fluctuations might destroy the bound excitonic condensate and the system settles in either the semimetal or the semiconducting state depending on the Coulomb interaction is small or large. The BCS–BEC crossover of the excitonic condensation state slightly deviates from the semimetal–semiconductor transition. The BCS-excitonic condensate thus attributes the simultaneous formation and condensation of the loosen electron–hole pairs found in the vicinity of the Fermi surface if the temperature is smaller than a critical value. Otherwise, one finds the BEC-excitonic condensate such as a condensation state of the preformed excitons in the semiconducting side by lowering the temperature. In the adiabatic regime, the contribution of the phonon modes has enhanced the electron–hole constraint. The excitonic transition temperature thus is enlarged as lowering the phonon frequency. In the opposite case with large phonon frequency, the assistance of the phonon becomes less important and the situation returns the purely electronic cases [6, 7, 25, 34].

## 6. Conclusion

To conclude, in this paper, we have analysed the static excitonic susceptibility function for the EFKM involving the electron–phonon interaction by adapting the random phase approximation. The excitonic condensate and its fluctuations in the semimetal/semiconducting materials are then discussed. Our results have illustrated the complex phase structure occurring in the systems. In the ground state, one finds a significant of the adiabatic phonon contribution in the formations and condensation of the excitons. In this adiabatic regime, the excitonic condensate might be found even without the Coulomb interaction. The excitonic condensation region suddenly expands as lowering the phonon frequency or enlarging the electron–phonon coupling. However, in the anti-adiabatic regime with large phonon frequency (in the comparison with the conduction electron hopping), the contribution of phonon becomes less important and the system exhibits a pure electronic situation. BCS–BEC crossover of the excitonic condensation state is also addressed. As increasing the electron–phonon coupling or decreasing the phonon frequency in the adiabatic regime, the primary contribution of phonon shifts the crossover to greater values of the Coulomb attraction. Considering more meticulously dynamic properties and fluctuated natures of the excitonic condensate via analyzing the optical conductivity or dynamical excitonic susceptibility function for the extended models or designing an experimental setup to verify the results would be our worthwhile investigations in the future.

## Acknowledgments

This work is funded by Ministry of Education and Training, Vietnam, under Grant Number B2021-MDA-14.

## Data availability statement

All data that support the findings of this study are included within the article (and any supplementary files).

## ORCID iDs

Van-Nham Phan https://orcid.org/0000-0003-0009-3932

## References

[1] Moskalenko S A and Snoke D W 2000 *Bose–Einstein Condensation of Excitons and Biexcitons and Coherent Nonlinear Optics with Excitons* (Cambridge: Cambridge University Press)
[2] Mott N F 1961 The transition to the metallic state *Phil. Mag.* **6** 287
[3] Knox R 1963 *Solid State Physics* ed F Seitz and D Turnbull (New York: Academic) p 100
[4] Kohn W 1968 Metals and insulators *Many Body Physics* ed C de Witt and R Balian (New York: Gordon & Breach)
[5] Bronold F X and Fehske H 2006 Possibility of an excitonic insulator at the semiconductor–semimetal transition *Phys. Rev.* B **74** 165107
[6] Ihle D, Pfafferott M, Burovski E, Bronold F X and Fehske H 2008 Bound state formation and the nature of the excitonic insulator phase in the extended Falicov–Kimball model *Phys. Rev.* B **78** 193103
[7] Phan V-N, Becker K W and Fehske H 2010 Spectral signatures of the BCS–BEC crossover in the excitonic insulator phase of the extended Falicov–Kimball model *Phys. Rev.* B **81** 205117
[8] Zenker B, Ihle D, Bronold F X and Fehske H 2012 Electron—hole pair condensation at the semimetal—semiconductor transition: a BCS—BEC crossover scenario *Phys. Rev.* B **85** 121102(R)
[9] Wachter P 2018 Exciton condensation and superfluidity in $TmSe_{0.45}Te_{0.55}$ *Adv. Mater. Phys. Chem.* **08** 120
[10] Kogar A *et al* 2017 Signatures of exciton condensation in a transition metal dichalcogenide *Science* **358** 1314
[11] Kim K, Kim H, Kim J, Kwon C, Sung Kim J and Kim B J 2021 Direct observation of excitonic instability in $Ta_2NiSe_5$ *Nat. Commun.* **12** 1969
[12] Wachter P, Bucher B and Malar J 2004 Possibility of a superfluid phase in a Bose condensed excitonic state *Phys. Rev.* B **69** 094502
[13] Cercellier H *et al* 2007 Evidence for an excitonic insulator phase in 1T−$TiSe_2$ *Phys. Rev. Lett.* **99** 146403
[14] Zenker B, Fehske H, Beck H, Monney C and Bishop A R 2013 Chiral charge order in 1T−$TiSe_2$: importance of lattice degrees of freedom *Phys. Rev.* B **88** 075138
[15] Lu Y F, Kono H, Larkin T I, Rost A W, Takayama T, Boris A V, Keimer B and Takagi H 2017 Zero-gap semiconductor to excitonic insulator transition in $Ta_2NiSe_5$ *Nat. Commun.* **8** 14408
[16] Volkov P A, Ye M, Lohani H, Feldman I, Kanigel A and Blumberg G 2021 Critical charge fluctuations and emergent coherence in a strongly correlated excitonic insulator *npj Quantum Mater.* **6** 52
[17] Zhang Y-S, Bruin J A N, Matsumoto Y, Isobe M and Takagi H 2021 Thermal transport signatures of the excitonic transition and associated phonon softening in the layered chalcogenide $Ta_2NiSe_5$ *Phys. Rev.* B **104** L121201
[18] Ye M, Volkov P A, Lohani H, Feldman I, Kim M, Kanigel A and Blumberg G 2021 Lattice dynamics of the excitonic insulator $ta_2Ni(Se_{1-x}S_x)_5$ *Phys. Rev.* B **104** 045102
[19] Subedi A 2020 Orthorhombic-to-monoclinic transition in $Ta_2NiSe_5$ due to a zone-center optical phonon instability *Phys. Rev. Mater.* **4** 083601
[20] Sugimoto K, Nishimoto S, Kaneko T and Ohta Y 2018 Strong coupling nature of the excitonic insulator state in $Ta_2NiSe_5$ *Phys. Rev. Lett.* **120** 247602
[21] Ejima S, Lange F and Fehske H 2021 Finite-temperature photoemission in the extended Falicov–Kimball model: a case study for $Ta_2NiSe_5$ *SciPost Phys.* **10** 77
[22] Do T-H-H, Bui D-H and Phan V-N 2017 Phonon effects in the excitonic condensation induced in the extended Falicov–Kimball model *Europhys. Lett.* **119** 47003
[23] Do T-H-H, Nguyen H-N and Phan V-N 2019 Thermal fluctuations in the phase structure of the excitonic insulator charge density wave state in the extended Falicov–Kimball model *J. Electron. Mater.* **48** 2677
[24] Zenker B, Ihle D, Bronold F X and Fehske H 2011 Slave-boson field fluctuation approach to the extended Falicov–Kimball model: charge, orbital, and excitonic susceptibilities *Phys. Rev.* B **83** 235123
[25] Phan V-N, Fehske H and Becker K W 2011 Excitonic resonances in the 2D extended Falicov–Kimball model *Europhys. Lett.* **95** 17006
[26] Seki K *et al* 2014 Excitonic Bose–Einstein condensation in $Ta_2NiSe_5$ above room temperature *Phys. Rev.* B **90** 155116
[27] Kim M-J, Schulz A, Takayama T, Isobe M, Takagi H and Kaiser S 2020 Phononic soft mode behavior and a strong electronic background across the structural phase transition in the excitonic insulator $Ta_2NiSe_5$ *Phys. Rev. Res.* **2** 042039(R)
[28] Phan V-N, Becker K W and Fehske H 2013 Exciton condensation due to electron–phonon interaction *Phys. Rev.* B **88** 205123
[29] Do T-H-H, Nguyen H-N, Nguyen T-G and Phan V-N 2016 Temperature effects in excitonic condensation driven by the lattice distortion *Phys. Status Solidi* B **253** 1210
[30] Yan J *et al* 2019 Strong electron–phonon coupling in the excitonic insulator $Ta_2NiSe_5$ *Inorg. Chem.* **58** 9036
[31] Sugimoto K, Kaneko T and Ohta Y 2016 Microscopic quantum interference in excitonic condensation of $Ta_2NiSe_5$ *Phys. Rev.* B **93** 041105(R)
[32] Nakano A, Hasegawa T, Tamura S, Katayama N, Tsutsui S and Sawa H 2018 Antiferroelectric distortion with anomalous phonon softening in the excitonic insulator $Ta_2NiSe_5$ *Phys. Rev.* B **98** 045139
[33] Wachter P and Bucher B 2013 Exciton condensation and its influence on the specific heat *Physica* B **408** 51
[34] Zenker B, Ihle D, Bronold F X and Fehske H 2010 Existence of excitonic insulator phase in the extended Falicov–Kimball model: SO(2)-invariant slave-boson approach *Phys. Rev.* B **81** 115122